J Fluoresc (2011) 21:1461–1466
DOI 10.1007/s10895-010-0831-x

ORIGINAL PAPER

Spectroscopic Properties, Energy Transfer and Structural Analysis of Sr_2CeO_4:M^+ and Sr_2CeO_4:Eu^{3+}, M^+ (M^+ = Li^+, Na^+, K^+)

Li-Li Shi · Cheng-Yu Li · Qiang Su

Received: 2 November 2010 / Accepted: 30 December 2010 / Published online: 29 January 2011

Abstract The room-temperature luminescent emission characteristics of Sr_2CeO_4:M^+ and Sr_2CeO_4:Eu^{3+},M^+ (M^+ = Li^+, Na^+, K^+) have been investigated under UV excitation. By introducing appropriate alkali metal cations dopants (Li^+, Na^+, K^+) into the crystalline lattice, not only emission color of the blue-white-emitting Sr_2CeO_4 doped with low Eu^{3+} content can be tuned to green, but also the red emission intensity of Sr_2CeO_4 doped with high Eu^{3+} concentration is strengthened significantly. The relevant mechanisms have been elucidated in detail.

Keywords Sr_2CeO_4 · Eu^{3+} · Photoluminescence · Energy transfer · Oxygen vacancy

Introduction

Materials based on Ceria (CeO_2) have been extensively investigated due to their broad applications in the fields of catalysis [1, 2] and optics [3], e.g., employed as promoters in Three Way Catalysts, as electrolyte or electrode promoters, active supports or cocatalysts, as well as energy transfer medium in phosphors to sensitize the luminescence of Pr^{3+}. Added with 2Sr (II), CeO_2 can form a novel type of solid solution Sr_2CeO_4, which can emit efficient blue light while irradiated by UV light, cathode ray or X-ray [4]. Its luminescence was generally considered to originate from a ligand-to-metal $O^{2-} \rightarrow Ce^{4+}$ charge transfer state (CTS) [4, 5]. Since it is an active center with 100% concentration, intensive studies on this phosphor have been focused on its synthesis [6, 7], structure [8, 9], emission mechanism [10, 11] and its potential applications, such as the employment in field emission displays [6]. Besides, Sr_2CeO_4 as a prominent host material for the incorporation of many trivalent luminescence centers, such as Eu^{3+}, Sm^{3+}, Dy^{3+}, Ho^{3+}, Er^{3+}, Tm^{3+}, etc., continues to attract a lot of attention from researchers [12–14]. Effective energy transfer from Ce^{4+}-O^{2-} CTS to these activation centers has been proposed to be responsible for their luminescence in Sr_2CeO_4 [15]. Among the many rare earth ions, Eu^{3+} with $4f^6$ electronic configuration can exhibits abundant emission colors, such as blue from $^5D_2$, green from $^5D_1$, red from $^5D_0$, which have been playing important roles in modern lighting and display fields. These characteristics of Eu^{3+} ions motivate researchers to explore the luminescence properties of Eu^{3+}-activated Sr_2CeO_4 most. When Eu^{3+} concentration becomes higher, emission from the Ce^{4+}-O^{2-} CTS will be much less until it disappears and then the emission owing to the Eu^{3+} transitions dominates finally. Correspondingly, emission colors of Sr_2CeO_4 added with different Eu^{3+} content changes from blue to red, in favor of their potential applications in low pressure mercury vapor (lpmv), high pressure mercury vapor (hpmv) lamps and TV tubes [16]. Our interests in Sr_2CeO_4:Eu^{3+} are heightened by the prospects in the application fields declared above.

In this work, the following two objectives can be achieved by way of introducing monovalent alkali metal ions (Li^+, Na^+, K^+) into Sr_2CeO_4:Eu^{3+}. On the one hand, emission color can be tuned for Sr_2CeO_4 doped with very low amount of Eu^{3+}, by adding cheaper carbonates instead of much more expensive europium oxide. On the other hand, the luminescence efficiency of the promising red-emitting material Sr_2CeO_4:Eu^{3+} can be enhanced by Li, Na or K addition.

L.-L. Shi · C.-Y. Li (✉) · Q. Su
State Key Laboratory of Rare Earth Resource Utilization,
Changchun Institute of Applied Chemistry,
Chinese Academy of Sciences,
Changchun 130022, People's Republic of China
e-mail: cyli@ciac.jl.cn

And then the possible mechanisms for the excellent effects of Li-/Na-/K-doping are discussed in detail.

Experimental

The stoichiometric compositions of samples are $Sr_{2-x}Eu_xM_{0.3}CeO_{4.15+x/2}$ (x=0, 0.005, 0.3, M^+ = Li^+, Na^+, K^+). They will be denoted as SCOE-X, SCOE-X-L, SCOE-X-N, SCOE-X-K, respectively, where X is the molar fraction of 10Eu(III). The solid-state reaction at high temperature has been employed for the synthesis of all samples. Reagents $SrCO_3$, Li_2CO_3, Na_2CO_3, K_2CO_3, CeO_2 (99.99%) and Eu_2O_3 (99.99%) were used as raw materials. All carbonates employed are analytical grade. The raw materials were blended and ground in an agate mortar. Then the mixture was heated at 1323 K in air in an alumina crucible for 10 h. After cooling to room temperature, each sample was re-ground again and the same procedure described above was adopted for them.

X-ray power diffraction spectra were collected using a Rigaku D/max-IIB X-Ray Diffractometer with Cu Kα (λ= 1.5405 Å) radiation, to certify that the prepared materials belong to Sr_2CeO_4 structure. The photoluminescence emission (PL) spectra of all samples were measured by a Fluorolog 3-21 spectrofluorometer (Jobin Yvon Inc/specx) equipped with a 450 W Xe lamp and double excitation monochromators. The luminescence decay curves were obtained at an Edinburgh FLS920 combined fluorescence lifetime and steady-state spectrometer. All the measurements were performed at room temperature.

Results and Discussions

Structural Characterization

In order to characterize the phase purity of all samples, X-ray powder diffraction (XRD) measurements were performed for the as-synthesized samples. X-ray diffraction data of $Sr_{2-x}Eu_xM_{0.3}CeO_{4.15+x/2}$ (x=0, 0.005, 0.3, M^+ = Li^+, Na^+, K^+) are given in parts (a), (b) and (c) of Fig. 1, which are in good agreement with the data in JCPDS standard card numbered 50-0115 [Sr_2CeO_4]. This confirms the formation of single-phase crystalline products. Sr_2CeO_4 is indexed to be an orthorhombic cell in space group *Pbam* [4]. The structure consists of linear chains of edge-sharing CeO_6 octahedra. The terminal Ce-O distance is about 0.1 Å shorter than the equatorial distance [4]. In the Sr_2CeO_4 structure, both the Ce^{4+} and Sr^{2+} ions is surrounded by six oxygen ions. Different from the former who occupies two nonequivalent positions, the latter occupies just one equivalent position. As we know, when coordination number amounts to 6, the ionic radii of cations Ce^{4+}, Eu^{3+}, Sr^{2+}, Li^+, Na^+ and K^+ are 87, 94.7, 118, 76, 102 and 138 pm, respectively [17]. Therefore, we believe that Eu^{3+} ions prefer to occupy both the Sr^{2+} sites and Ce^{4+} sites because of the similar radius and charge.

Effect of the incorporation of Li^+ ions on $SrTiO_3$ structure has been investigated in Ref. [18]. The authors considered it was not likely for Li^+ ion to be located in Ti^{4+}

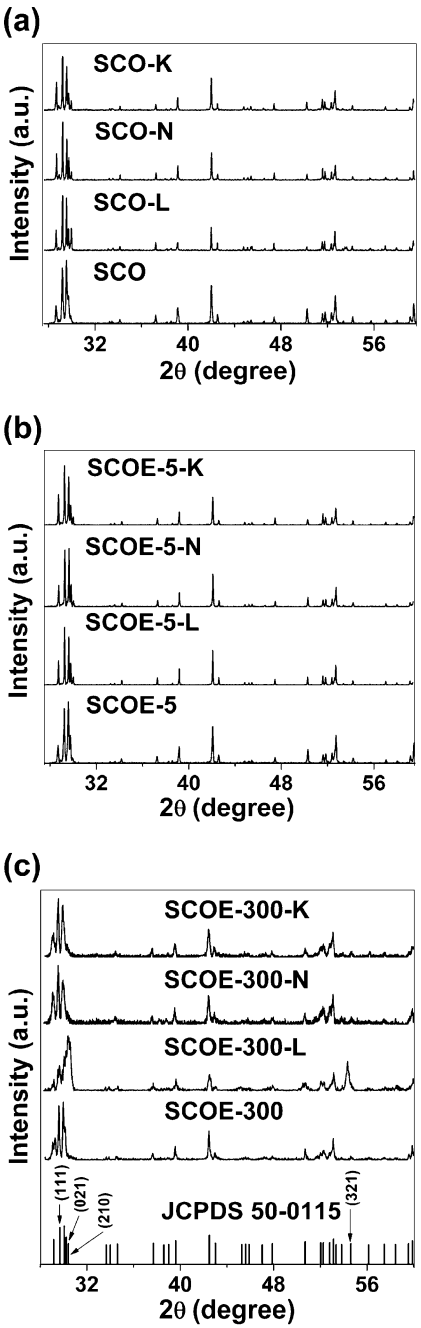

Fig. 1 X-ray diffraction patterns of $Sr_{2-x}Eu_xM_{0.3}CeO_{4.15+x/2}$ (x=0, 0.005, 0.3, M^+ = Li^+, Na^+, K^+). **a** x=0, SCO and SCO-M; **b** x=0.005, SCOE-5 and SCOE-5-M; **c** x=0.3, SCOE-300 and SCOE-300-M

site because of the big charge difference between them. However, we believe that Li^+ ion is small enough to occupy any crystal lattice site. In our present research, when introduced into SCO, the Li^+ ions could be located at the sites of Sr^{2+} and Ce^{4+}, moreover, there is a possibility that a number of Li^+ ions reside in interstitial sites between or among the host ions. For Na^+ ions, they could be located at Sr^{2+} sites more easily than Ce^{4+} sites, but it is difficult for K^+ ions to replace Sr^{2+} or Ce^{4+} because of their bigger radii.

In part (c) of Fig. 1, note that the representative diffraction data of Eu-rich material (SCOE-300) doped with Li^+ ions are obviously different from others. In SCOE-300-L, the relative intensity of crystal faces (0 2 1), (2 1 0) and (3 2 1) increase, but the relative intensity of crystal face (1 1 1) decreases. We think this observation can be assigned to the enormous changes in lattice constants of this sample. The corresponding unit-cell constants and unit cell volumes of samples SCOE-300 and SCOE-300-L/N/K are listed in Table 1. Compared with another three samples, the largest expansion of the two cell constants *a*, *c* and the largest contraction of the cell constant *b* of the sample are observed in SCOE-300-L, accounting for the considerable variations in the relative intensity of the four crystal faces.

As we know, if the ions with smaller radius substitute the larger cations in the crystalline lattice, the cell volume of the host compound will decrease [19, 20]. Therefore, as shown in Table 1, the cell volume of SCOE-300-N decreases with the doping of Na^+ ions, because the ionic radii of Na^+ ions (102 pm) are smaller than that of Sr^{2+} ions (118 pm). This finding confirms that Na^+ ions prefer to occupy Sr^{2+} sites than Ce^{4+} sites, as discussed above. The same rule can also apply to SCOE-300-K, the cell volume of SCOE-300 increases when K^+ ions are added as charge compensation, which have bigger radius than Sr^{2+} ions. However, the cell volume of SCOE-300 doped with Li^+ increases, despite the fact that the Li^+ is smaller than Sr^{2+} or Ce^{4+}. The larger size of Li^+ ions than that of interstitial sites would be responsible for this phenomenon.

Effect of $Li^+/Na^+/K^+$ on Emission Spectra of SCO

Figure 2 demonstrates the CT luminescent behaviors of Ce^{4+} in SCO doped with Li^+, Na^+ or K^+ ions. Note that the PL

Table 1 The calculated lattice parameters of SCOE-300 doped with Li^+, Na^+ or K^+

Phosphors	a (nm)	b (nm)	c (nm)	V (nm^3)
SCOE-300	0.61174	1.03968	0.36024	0.22852
SCOE-300-L	0.61242	1.03591	0.36057	0.22875
SCOE-300-N	0.61014	1.03717	0.35976	0.22766
SCOE-300-K	0.61210	1.03714	0.36055	0.22889

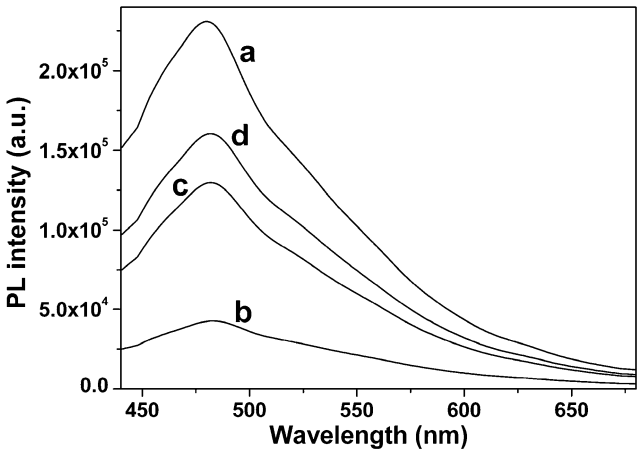

Fig. 2 Photoluminescence emission spectra of un-doped SCO and SCO doped with M^+ ions. **a** SCO; **b** $M^+ = Li^+$; **c** $M^+ = Na^+$; **d** $M^+ = K^+$

intensity of the Ce-O CTS at about 480 nm drops in the following order: SCO > SCO-K > SCO-N > SCO-L. In other words, the addition of Li^+, Na^+ or K^+ ions quenches the luminescence from the Ce-O CTS to a different degree.

The Ce^{4+}-O^{2-} charge transfer state, like the Eu^{3+}-O^{2-} CTS [21], means not only an electron is transferred from O^{2-} ion to the $4f^0$ shell of Ce^{4+} ion but also a hole moves from a Ce^{4+} ion to an oxygen ligand. Further studies on the formation of the charge transfer state were carried out in the Y_2O_3-Yb and Lu_2O_3-Yb crystals [22], which demonstrated that the hole preferred to be completely delocalized on a single ligand O^{2-} ion, rather than be delocalized among the ligands. This "delocalization effect" is suggested to be also applied to the hole on "Ce-O-Sr" or "Ce-O-Ce". Since the hole is localized in the 2p-shell of one of the oxygen ligands, it can be easily captured by the traps [23], like Mc_e''' or Ms_r' ($M^+ = Li^+$, Na^+, K^+). With delocalization and capture of the holes, the wave function overlaps between the holes on the ligands and the electrons on the Ce^{3+} ions becomes smaller. This can reasonably elucidate why the charge transfer (CT) transition probability involving Ce^{4+} has shown a descending trend with the addition of these monovalent co-dopants.

Furthermore, when different monovalent alkali metals are added into the SCO crystal lattice, they cause diverse chemical reactions [24, 25]. For Li^+ doping, there may exist the following three reactions: $Li^{\bullet} \rightarrow Li'_{Sr} + V_o^{\bullet\bullet}$, $Li^{\bullet} \rightarrow Li'''_{Ce} + 2V_o^{\bullet\bullet}$ and $Li^{\bullet} \rightarrow Li_i^{\bullet}$. Similarly, possible chemical substitution mechanisms of Na^+ doping are $Na^{\bullet} \rightarrow Na'_{Sr} + V_o^{\bullet\bullet}$ and $Na^{\bullet} \rightarrow Na'''_{Ce} + 2V_o^{\bullet\bullet}$. However, there may exist only one chemical reaction for K^+ doping as follows: $K^{\bullet} \rightarrow K'_{Sr} + V_o^{\bullet\bullet}$. Therefore, it is easy to understand that the capability for the traps generated by the doping of Li^+, Na^+ and K^+ to

capture holes weakens in the following order: $Li^+ > Na^+ > K^+$, in good agreement with the sequence observed in Fig. 2.

Effect of $Li^+/Na^+/K^+$ on Emission Spectra of SCOE-5 and Energy Migration Between Ce^{4+} and Eu^{3+}

Under the longer ultraviolet (UV) (around 365 nm) excitation, the Eu-poor sample (x=0.005) shows a strong blue-white emission, consisting of a Ce-O broad band in the blue spectral region, a set of Eu^{3+} intra-$4f^6$ sharp lines in the blue/green/red regions, and the considerable overlaps between them in the whole region. With the addition of Li^+, Na^+ and K^+ ions, the Ce-O CT luminescence in SCOE-5 is dramatically quenched, behaving similarly to the observation in SCO. Different from the blue emission, with the incorporation of Li^+, Na^+ and K^+ ions, the red emission coming from $^5D_0$-$^7F_2$ increases by a factor of 1.94, 1.57 and 1.34, respectively. The CIE chromaticity coordinates of phosphors are calculated to be x=0.1806, y=0.2664 for SCOE-5, x=0.2365, y=0.3808 for SCOE-5-L, x=0.2565, y=0.4234 for SCOE-5-N, and x=0.2193, y=0.3415 for SCOE-5-K, respectively. Accordingly, emission colors of samples vary from blue-white to green. As a reference [16], with increasing Eu^{3+} doping concentration, Sr_2CeO_4:Eu^{3+} phosphors could behave in a similar way. Different from the cheaper alkali metal ions used in the former, much more expensive europium oxide as raw materials were employed in the prepared procedures of Sr_2CeO_4:Eu^{3+}, which was not conducive to lower costs.

Figure 4 shows the Ce-O CT luminescence decay curves of the Eu-poor powders doped with Li^+, Na^+ or K^+, recorded at room temperature. It can be seen from Fig. 4 (a) that SCOE-5 and SCOE-5-L follow single exponential time dependencies with time constants of 54.4 and 28.8 μs, respectively. For SCOE-5-N and SCOE-5-K, the decay curves can be well fitted into double-exponential functions, the fitting results are shown inside of Fig. 4 (b) and (c). Both of them have two lifetimes, a fast one and a short one. The average lifetimes for the host lattice emission in SCOE-5-N and SCOE-5-K, defined as $t = (A_1t_1^2 + A_2t_2^2)/(A_1t_1 + A_2t_2)$ [26, 27], are calculated to be 28.9 and 32.0 μs, respectively. Note that the PL decay time for the Ce-O CT luminescence decreases with the addition of Li^+, Na^+ and K^+, demonstrating that energy transfer from the Ce-O CTS to Eu^{3+} could be improved by means of adding appropriate alkali metal ions [12].

In summary, with the introduction of M^+ ($M^+ = Li^+$, Na^+, K^+) in the Eu-poor system (SCOE-5), we have observed luminescence quenching of the Ce-O CTS (Fig. 3), remarkable enhancement of luminescence from Eu^{3+} $^5D_0$-$^7F_2$ transition (Fig. 3), as well as improved energy transfer from Ce^{4+} to Eu^{3+} (Fig. 4). (i) Firstly, we explain why energy migration is promoted, since it can influence

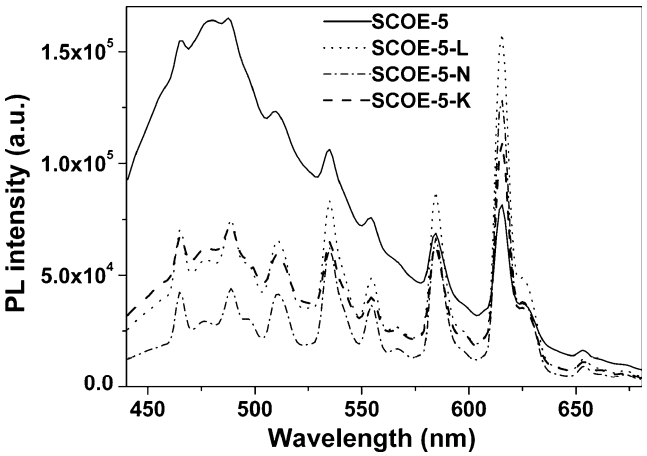

Fig. 3 Photoluminescence emission spectra of M-free and M-doped SCOE-5 ($M^+ = Li^+$, Na^+, K^+)

another two phenomena. From the chemical reactions listed above, the creation of oxygen vacancies seems to be the dominant incorporation mechanism. As a result, these oxygen vacancies, which can act as sensitizers [28–30], facilitate the strong mixing of the Ce-O and Eu-O charge transfer states, and thus promote energy migration from the Ce-O CTS to Eu^{3+}. Furthermore, the more oxygen vacancies generated by doping ions, the more effective energy transfer happens between Ce^{4+} and Eu^{3+} ions. (ii) Secondly, for luminescence quenching of the Ce-O CTS, it is not only for the smaller wave function overlap between the holes on the ligands O^- and the electrons on the Ce^{3+} ions but also because of promotion of energy transfer from the Ce-O CTS to Eu^{3+} ions. (iii) Finally, we have given reasons why large increases in emission intensity can be observed for the peak at 616 nm in SCOE-5. It is considered that the improved energy transfer should be mainly responsible for the results achieved. Furthermore, alkali-metals doping have different effects on energy transfer ($Li^+ > Na^+ > K^+$), which is in line with the sequence of luminescence from Eu^{3+} $^5D_0$-$^7F_2$ transition.

Effect of $Li^+/Na^+/K^+$ on Emission Spectra of SCOE-300

Figure 5 presents the emission spectra of the promising red-emitting materials SCOE-300 (x=0.3) doped with Li^+, Na^+ and K^+. Under 365 nm Hg-line excitation, the main emission peaks located at about 591, 616 and 654 nm, are observed for SCOE-300, which come from the $^5D_0 \rightarrow {}^7F_1$, $^7F_2$ and $^7F_3$ transitions of Eu^{3+}, respectively. By comparing the emission spectra of all samples, we note that, with the incorporation of Li^+, Na^+ and K^+, the emission intensity of the Eu^{3+} $^5D_0$-$^7F_2$ transition for M^+-doped SCOE-300 ($M^+ = Li^+$, Na^+, K^+) increases by 154%, 209% and 57%, respectively. Obviously, in SCOE-300, the addition of Na^+

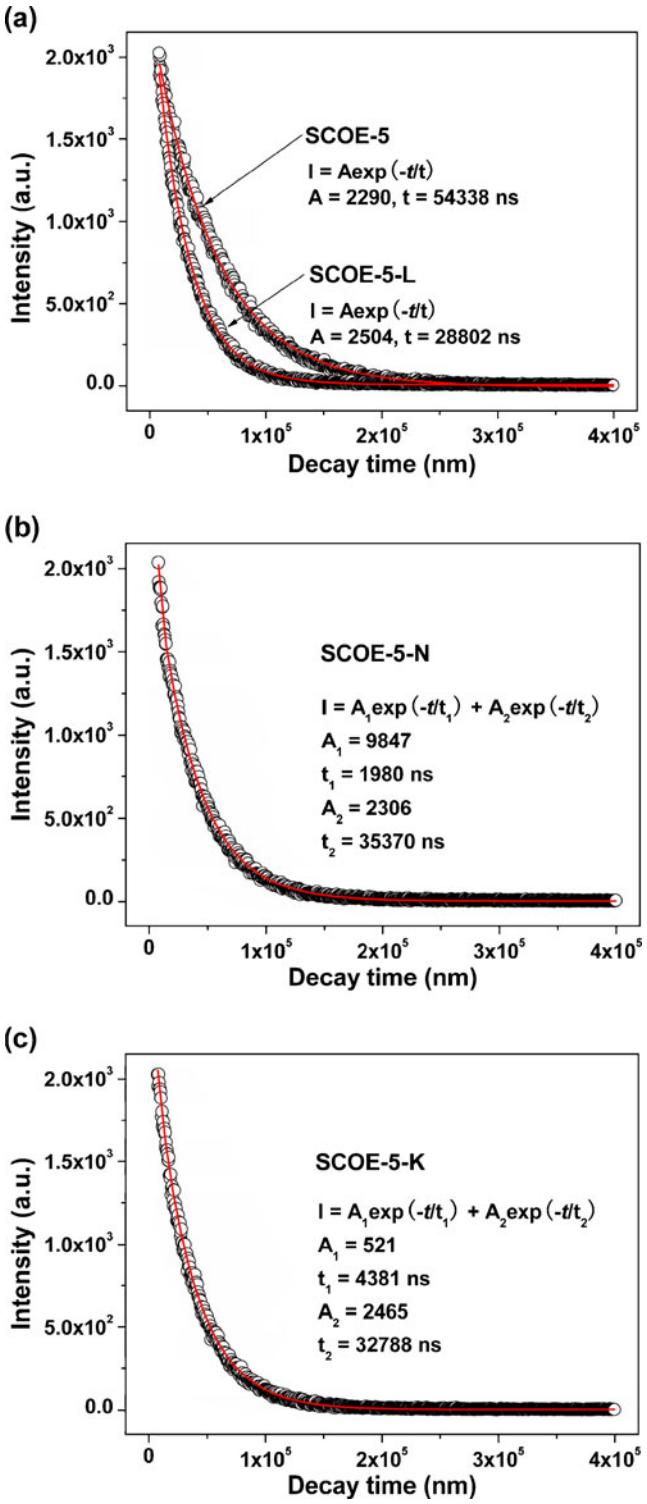

Fig. 4 Luminescence decay curves for the Ce-O charge transfer state of M^+-free and M^+-doped SCOE-5 ($M^+ = Li^+, Na^+, K^+$). Round circles typify the experimental data, red solid lines indicate the fitting results. The excitation was done at 340 nm and the emission was monitored at 480 nm

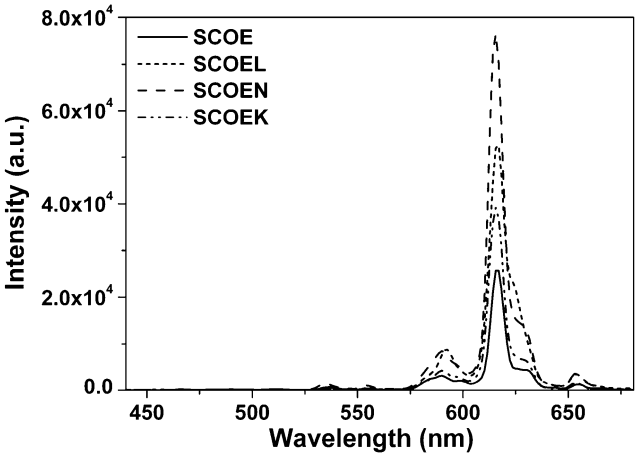

Fig. 5 Photoluminescence emission spectra of M-free and M-doped SCOE-300 ($M^+ = Li^+, Na^+, K^+$)

ions can heighten the emission intensity of the $^5D_0$-$^7F_2$ peak much more than Li^+ and K^+ ions. These findings can be explained in terms of the following two aspects.

On the one hand, promotion of energy transfer from the Ce-O CTS to Eu^{3+} by Li-/Na-/K-addition contributes to the higher brightness of SCOE-300, which should obey SCOE-300-L > SCOE-300-N > SCOE-300-K > SCOE-300. On the other hand, the information about the symmetry at the site of the Eu^{3+} ions should be considered in the Eu-copious material, because the hypersensitive $^5D_0$-$^7F_2$ transition is strongly dependent on the Eu^{3+} ion surroundings [31]. Generally, the intensity ratio R of the transitions $^5D_0$-$^7F_2$ to $^5D_0$-$^7F_1$ is considered to be a good measure for the symmetry of Eu^{3+} site [32, 33]. Here, the intensity of the transitions $^5D_0$-$^7F_2$ and $^5D_0$-$^7F_1$ is defined as the area under their PL curves calculated by integrating from 604 to 644 and from 572 to 604 nm, respectively. The R values calculated for samples SCOE-300, SCOE-300-L, SCOE-300-N and SCOE-300-K are 4.79, 5.54, 5.80 and 5.97, respectively. The higher the R value, the higher will be the asymmetry around Eu^{3+}. Therefore, the addition of Li^+, Na^+ and K^+ renders the Sr_2CeO_4 host structure towards lower symmetry in turn and finally the larger transition probability for the enforced electric-dipole allowed $^7F_2$ transition. In other words, according to this deduction, the $^5D_0$-$^7F_2$ intensity should increase in the following order: SCOE-300-L < SCOE-300-N < SCOE-300-K. To sum up, the different effects of doping ions on energy transfer and the local symmetry surrounding Eu^{3+} ions finally result in the observations in Fig. 5.

Conclusions

In conclusion, the considerable influences of Li^+, Na^+ and K^+ ions on the emission spectra of Sr_2CeO_4 (SCO) and Eu-

poor/rich SCO have been investigated at room temperature. For Eu-poor material (SCOE-5), its emission color changed from blue-white to green with the incorporation of co-dopants, as a result of the quenched host lattice emission plus the improved red emission of Eu^{3+} ions. For Eu-rich phosphor (SCOE-300), its high-purity red emission was greatly intensified by co-doping of Eu^{3+} and $Li^+/Na^+/K^+$. It is a reasonable explanation for these observations that $Li^+/Na^+/K^+$ incorporation can generate oxygen vacancies to promote energy transmission from Ce^{4+} to Eu^{3+}, reduce the environmental symmetry around Eu^{3+}, and cause hole traps to quench the Ce-O CT luminescence. These green and red materials might be strong candidates for display applications in the future.

Acknowledgements The financial support for this work was extended by National Basic Research Program of China (2007CB935502) and National Natural Science Foundation of China (Grant No. 20921002).

References

1. Montini T, Speghini A, Rogatis LD, Lorenzut B, Bettinelli M, Graziani M, Fornasiero P (2009) Identification of the structural phases of $Ce_xZr_{1-x}O_2$ by Eu(III) luminescence studies. J Am Chem Soc 131:13155–13160
2. Esch F, Fabris S, Zhou L, Montini T, Africh C, Fornasiero P, Comelli G, Rosei R (2005) Electron localization determines defect formation on Ceria substrates. Science 309:752–755
3. Yan B, Cai XW, Xiao XZ (2009) Photoluminescence enhancement effect of CeO_2 in rare earth composites $MM'O_3/CeO_2$ and $MM'O_3/CeO_2:Pr^{3+}$ (M=Ca, Sr; M′=Ti, Zr). J Fluoresc 19:221–228
4. Danielson E, Devenney M, Giaquinta DM, Golden JH, Haushalter RC, McFarland EW, Poojary DM, Reaves CM, Weinberg WH, Wu XD (1998) A rare-earth phosphor containing one-dimensional chains identified through combinatorial methods. Science 279:837–839
5. Pieterson LV, Soverna S, Meijerink A (2000) On the nature of the luminescence of Sr_2CeO_4. J Electrochem Soc 147:4688–4691
6. Jiang YD, Zhang FL, Summers CJ, Wang ZL (1999) Synthesis and properties of Sr_2CeO_4 blue emission powder phosphor for field emission displays. Appl Phys Lett 74:1677–1679
7. Serra OA, Severino VP, Calefi PS, Cicillini SA (2001) The blue phosphor Sr_2CeO_4 synthesized by Pechini's method. J Alloy Compd 323–324:667–669
8. Ghildiyal R, Page P, Murthy KVR (2007) Synthesis and characterization of Sr_2CeO_4 phosphor: positive features of sol–gel technique. J Lumin 124:217–220
9. Yu XB, He XH, Yang SP, Yang XF, Xu XL (2003) Synthesis and luminescence of Sr_2CeO_4 superfine particles by citrate-gel method. Mater Lett 58:48–50
10. Park CH, Kim CH, Pyun CH, Choy JH (2000) Luminescence of Sr_2CeO_4. J Lumin 87–89:1062–1064
11. Lu CH, Chen CT (2007) Luminescent characteristics and microstructures of Sr_2CeO_4 phosphors prepared via sol–gel and solid-state reaction routes. J Sol Gel Sci Technol 43:179–185
12. Hirai T, Kawamura Y (2004) Preparation of Sr_2CeO_4 blue phosphor particles and rare earth (Eu, Ho, Tm, or Er)-doped Sr_2CeO_4 phosphor particles, using an emulsion liquid membrane system. J Phys Chem B 108:12763–12769
13. Nag A, Kutty TRN (2003) Photoluminescence of $Sr_{2-x}Ln_xCeO_{4+x/2}$ (Ln=Eu, Sm or Yb) prepared by a wet chemical method. J Mater Chem 13:370–376
14. Xiao XZ, Yan B (2008) $Sr_2CeO_4:Eu^{3+}$ and Sr_2CeO_4:5 mol% Eu^{3+}, 3 mol% Dy^{3+} microphosphors: wet chemistry synthesis from hybrid precursor and photoluminescence properties. J Phys Chem Solids 69:1665–1668
15. Viagin O, Masalov A, Ganina I, Malyukin Y (2009) Mechanism of energy transfer in $Sr_2CeO_4:Eu^{3+}$ phosphor. Opt Mater 31:1808–1810
16. Sankar R, Subba Rao GV (2000) Eu^{3+} luminescence, $Ce^{4+} \rightarrow Eu^{3+}$ energy transfer, and white-red light generation in Sr_2CeO_4. J Electrochem Soc 147:2773–2779
17. Shannon RD (1976) Revised effective ionic radii and systematic studies of interatomic distances in halides and chalcogenides. Acta Cryst A 32:751–767
18. Tian LH, Mho SI (2003) Enhanced luminescence of $SrTiO_3:Pr^{3+}$ by incorporation of Li^+ ion. Solid State Commun 125:647–651
19. Hannan A, Iwasa K, Kohgi M, Suzuki T (2000) Crystal-lattice anomaly of CeSb under high pressure induced by magnetic polaron formation. J Phys Soc Jpn 69:2358–2359
20. Ahmed MA, Ateia E, EI-Dek SI (2003) Rare earth doping effect on the structural and electrical properties of Mg–Ti ferrite. Mater Lett 57:4256–4266
21. Fonger WH, Struck CW (1971) Energy loss and energy storage from the Eu^{+3} charge-transfer states in Y and La oxysulfides. J Electrochem Soc 118:273–280
22. Krasikov D, Mikhailin V, Scherbinin A (2009) Ab initio embedded cluster calculations of the electronic structure and properties of the Yb charge transfer luminescence centres. Phys Procedia 2:559–565
23. Hoshina T, Imanaga S, Yokono S (1977) Charge transfer effects on the luminescent properties of Eu^{3+} in oxysulfides. J Lumin 15:455–471
24. Yang SH, Yokoyama M (1998) The effect of Ni, Cu and Zn doping on the luminance and conductivity of blue $ZnGa_2O_4$ phosphor. Jpn J Appl Phys 37:6429–6433
25. Kroger FA, Vink HJ (1956) In: Seitz F, Turnbull D (eds) Solid state physics. Academic, New York, p 307
26. Fujii T, Kodaira K, Kawauchi O, Tanaka N (1997) Photochromic behavior in the fluorescence spectra of 9-Anthrol encapsulated in Si-Al glasses prepared by the Sol-Gel method. J Phys Chem B 101:10631–10637
27. Liu XM, Pang R, Quan ZW, Yang J, lin J (2007) Tunable luminescence properties of Tb^{3+}-Doped $LaGaO_3$ nanocrystalline phosphors. J Electrochem Soc 154:J185–J189
28. Gu F, Li CZ, Jiang HB (2006) Combustion synthesis and photoluminescence of $MgO:Eu^{3+}$ nanocrystals with Li^+ addition. J Cryst Growth 289:400–404
29. Yi SS, Bae JS, Shim KS, Jeong JH, Park JC, Holloway PH (2004) Enhanced luminescence of Gd2O3:Eu3+ thin-film phosphors by Li doping. Appl Phys Lett 84:353–355
30. Yi SS, Shim KS, Yang HK, Moon BK, Choi BC, Jeong JH, Kim JH, Bae JS (2007) Improved cathodoluminescent characteristics of $Y_2O_3:Eu^{3+}$ thin films by Li-doping. Appl Phys A 87:667–671
31. Rosa ILV, Olivera LH, Longo E, Varela JA (2010) Synthesis and photoluminescence behavior of the Eu^{3+} ions as a nanocoating over a silica Stöber matrix. J Fluoresc. doi:10.1007/s10895-010-0671-8
32. Su YG, Li LP, Li GS (2008) Synthesis and optimum luminescence of $CaWO_4$-based red phosphors with codoping of Eu^{3+} and Na^+. Chem Mater 20:6060–6067
33. Guo CF, Ding X, Xu Y (2010) Luminescent properties of Eu^{3+}-Doped $BaLn_2ZnO_5$ (Ln=La, Gd, and Y) phosphors by the Sol–Gel method. J Am Ceram Soc 93:1708–1713